Published in final edited form as:
J Comp Neurol. 2013 July 1; 521(10): 2359–2372. doi:10.1002/cne.23289.

Corticospinal sprouting occurs selectively following dorsal rhizotomy in the macaque monkey

Corinna Darian-Smith[1], **Alayna Lilak**[2], and **Christina Alarcón**[3]

[1]Department of Comparative Medicine, 300 Pasteur Drive, Edwards Building, Stanford University School of Medicine, Stanford, CA 94305-5342 USA

[2]Department of Comparative Medicine, 300 Pasteur Drive, Edwards Building, Stanford University School of Medicine, Stanford, CA 94305-5342 USA

[3]University of California Davis School of Veterinary Medicine, One Shields Avenue, Davis, CA 95616, USA

Abstract

The corticospinal tract in the macaque and human forms the major descending pathway involved in volitional hand movements. Following a unilateral cervical dorsal root lesion, where sensory input to the first three digits (D1–D3) is removed, monkeys are initially unable to perform a grasp retrieval task requiring sensory feedback. Over several months, however, they recover much of this capability. Past studies in our lab have identified a number of changes in the afferent circuitry that occur as function returns, but do changes to the efferent pathways also contribute to compensatory recovery? In this study we examined the role of the corticospinal tract in pathway reorganization following a unilateral cervical dorsal rhizotomy. Several months after animals received a lesion, the corticospinal pathways originating in the primary somatosensory and motor cortex were labeled and terminal distribution patterns on the two sides of the cervical cord compared. Tracers were injected only into the region of D1–D3 representation (identified electrophysiologically). We observed a strikingly different terminal labeling pattern post-lesion for projections originating in the somatosensory versus motor cortex. The terminal territory from the somatosensory cortex was significantly smaller compared with the contralateral side (area mean = 0.30 vs 0.55mm^2), indicating retraction or atrophy of terminals. In contrast, the terminal territory from the motor cortex did not shrink and in 3 of 4 animals, aberrant terminal label was observed in the dorsal horn ipsilateral to the lesion, indicating sprouting. These differences suggest that cortical regions play a different role in post-injury recovery.

Keywords

spinal injury; dorsal root; nonhuman primate; reorganization; somatosensory cortex; motor cortex

INTRODUCTION

The corticospinal pathway (CST) in the macaque and human is the major descending pathway involved in fine voluntary hand movement, and its importance increases with the evolution of fractionated digit use in the primate. In macaques, as in humans, CST

Corresponding Author: Corinna Darian-Smith, Department of Comparative Medicine, 300 Pasteur Drive, Edwards Building Room R350, Stanford University School of Medicine, Stanford, CA 94305-5342, USA (650) 736 0969 ph, (650) 498 5085 fx, cdarian@stanford.edu.

Role of Authors: Study concept and design: CDS. Acquisition of data: primarily AL, but also CA and CDS. Analysis and interpretation of data: CDS, AL. Drafting of the manuscript: CDS. Obtained funding: CDS.

projections originate from a number of cortical areas, including the primary motor cortex, premotor and supplementary motor regions, the primary somatosensory cortex (S1), and the insular cortex (Galea and Darian-Smith, 1994; Darian-Smith et al., 1996; Lemon, 2008). Input to the cervical spinal cord from each cortical region is also unique in its pattern of termination and function (Ralston and Ralston, 1985; Lemon and Griffiths, 2005).

The CST from the motor cortex has been implicated in the recovery of hand function in macaque monkeys following hemisection lesions in the cervical spinal cord (Galea and Darian-Smith, 1997a,b; Rosenzweig et al., 2010). It has also been a focus of rodent studies interested in the CSTs regenerative potential following central injuries and various experimental manipulations, with variable success (Case and Tessier-Lavigne, 2005; Brus-Ramer et al., 2007; Garcia-Alias et al., 2009; Ghosh et al., 2010; Liu et al., 2010).

However, spontaneous changes in corticospinal projections from sensorimotor cortex following cervical dorsal rhizotomy (DRL) in the monkey have not been examined previously. Following a unilateral cervical DRL in the macaque, that removes input selectively from D1–D3, we have shown that (1) monkeys are initially unable to use their hands in a reach retrieval task requiring cutaneous feedback, but then recover this ability significantly over the first 1–3 months (Darian-Smith and Ciferri, 2005), (2) that this behavioral recovery is accompanied by local sprouting within the dorsal horn of small numbers of spared primary afferents (Darian-Smith, 2004), (3) that there is considerable and comparable reorganization of the representational maps of the digits at multiple levels of the neuraxis, including the cuneate nucleus and somatosensory cortex (Darian-Smith and Brown, 2000; Darian-Smith, 2009), and (4) that there is an increase in GABAergic synaptic profiles in the dorsal horn indicating major circuitry modification in this region (Darian-Smith et al., 2010). In this study we were interested in the role of the CST projections in the circuitry modifications that take place post-injury, since these pathways are likely to play a key role in the recovery of digit function, and the modulation of altered sensory input to the cervical spinal cord following a DRL. Our findings suggest that CST projections from the reorganized S1 and motor cortex play very different roles in post-injury spinal circuitry remodeling.

MATERIALS AND METHODS

Animals used and general procedures

Seven young adult male macaque monkeys (*Macaca fascicularis*), averaging 2.9 ±0.6 kg, were used in this study. All monkeys were colony bred and between 2.5–3.5 years of age (where sexual maturity is typically reached at 4 years in this species). Though the animals used in the present study were young, their sensorimotor pathways mediating hand function were mature, and their age is unlikely to have played a role in our findings. Monkeys were housed at the Stanford Research Animal Facility, in adapted four-unit cages per monkey (64 × 60 × 77 cm dwh per unit). All procedures were conducted in accordance with National Institutes of Health guidelines and approved by the Stanford University Institutional Animal Care and Use Committee. See Table 1 for details.

Experimental sequence

All animals underwent two surgeries. In the initial surgery a laminectomy was made to expose the cervical cord (C5-T1) to assess the distribution of sensory input from the first three digits of one hand (the thumb, index and middle fingers), and to then make a DRL. In the second surgery, performed 9–18 weeks later (see Table 1), a bilateral craniotomy was made over the primary somatosensory and primary motor cortex in the region of hand representation. This area was mapped electrophysiologically to locate the boundaries of D1–

D3, both on the side contralateral to the lesion, which was known to be reorganized following the DRL, and the non-lesioned side (ipsilateral to the lesion). The region of reorganization, which has been described in detail previously (Darian-Smith and Brown, 2000; Darian-Smith, 2004; Darian-Smith and Ciferri, 2006; Vessal et al., 2007; Vessal and Darian-Smith, 2010), was then used to place a series of 6–9 injections of either the anterograde tracer biotin dextran amine (BDA), or Lucifer yellow dextran (LYD) into the somatosensory or motor cortex. Within animals, an identical number of injections were made bilaterally. Table 1 specifies which tracer was used and where in each monkey (see also Figure 1). BDA was also injected into the motor (M602 and M603) or somatosensory cortex (M701), but due to tracer batch failure, these series were not included in the study and are not indicated in Table 1.

Surgery and perfusion

Anesthesia was first induced with ketamine hydrochloride (10 mg/kg) and animals were subsequently maintained throughout surgery with gaseous isoflurane (1–1.5%)/O_2 using a standard open circuit anesthetic machine. Atropine sulfate (0.05 mg/kg) and cefazolin (20 mg/kg) were administered i.m. i.v. prior to surgery respectively. A laminectomy was made during the first surgery in each monkey and the overlying dura cut to expose dorsal rootlets through segments C5–T1 (see Darian-Smith, 2004 for details). Electrophysiological recordings were made to create a microdermatome map as described earlier (Darian-Smith and Brown, 2000; Darian-Smith, 2004; Darian-Smith and Ciferri, 2005), and this was then used to select rootlets to cut. All rootlets with receptive fields on the first three digits were sectioned in 2 places (using iridectomy scissors) to remove 2–3 mm of the rootlet along the length of the lesion. The overlying tissues and skin were then carefully sutured closed in layers. Torbugesic (0.02 mg/kg, i.m.) was administered prior to final suturing to provide a postoperative analgesic, and monkeys returned to their cages to be observed closely. Typically these monkeys were awake and alert within a few hours, and no postoperative sequalae were observed.

In the second surgery, a bilateral craniotomy was made over the central sulcus so that recordings and tracer injections could be made (see below) to identify the boundaries of the D1–D3 representation. A small ~1cm^2 bone flap was removed and the dura resected. Once injections were complete, the bone flap was replaced and the overlying skin sutured. All anesthesia and postoperative analgesic regiment were as described for the laminectomy. Monkeys also recovered rapidly from this procedure.

At the end of each experiment, monkeys were deeply anesthetized and given a lethal dose (i.v.) of sodium pentobarbital (0.44 ml/kg) until spontaneous breathing and corneal reflex had ceased. Animals were then manually breathed and perfused transcardially with 0.1 M phosphate-buffered saline (PBS; pH 7.4, 1 liter) followed by 4% paraformaldehyde. The brain and spinal cord were removed, postfixed (same perfusate) for 4 hours, and transferred to 30% for cryoprotection.

Electrophysiological recordings in dorsal roots and cortex

Recordings were made from dorsal rootlets as described elsewhere (Darian-Smith and Brown, 2000; Darian-Smith, 2004; Darian-Smith and Ciferri, 2005). Briefly, a laminectomy was made and dura resected to expose rootlets from C5-T1, and the exposure photographed so that individual rootlets could be identified for accuracy. A tungsten microelectrode (1.2–1.4 mΩ at 1 kHz) was used to record from each rootlet, and 8–10 single or small multiunit extracellular recordings made from axons within each fascicle to produce a microdermatome map. Cutaneous receptive fields (RFs) were mapped with a combination of manipulation, a camel hair brush, and Von Frey hairs. The RF was defined as cutaneous if the stimulus force

of ≤ 2.0g evoked a response. When the stimulus force was greater than 2.0g, or where joint movement or hand manipulation was needed to evoke a response, the RF was marked as deep, and where there was ambiguity as to whether the RF was cutaneous or deep, the RF was included as cutaneous for the purposes of defining which rootlets to lesion. All RFs were mapped on to hand/body image score sheets and rootlets with cutaneous RFs mapped on the thumb, index, and middle fingers then cut.

Cutaneous RF maps of hand representation were also made bilaterally within the primary somatosensory cortex two weeks prior to the terminal experiment. A craniotomy was made and dura cut to expose a small window of cortex (about 1 cm^2), and electrode penetrations made along the rostral lip of the postcentral gyrus at the approximate border of areas 3b/1 (Figure 1). Extracellular small multi-unit recordings were made in the somatosensory cortex, using stimuli as described above for dorsal rootlets. Similar recordings have been described previously (Darian-Smith and Brown, 2000; Darian-Smith, 2004; Darian-Smith and Ciferri, 2005).

Tracing corticospinal terminal fields within the spinal cord

Anterograde tracers Biotin dextran amine (BDA,15% aqueous, Sigma, B-9139) or Lucifer Yellow dextran (LYD, 15% aqueous, Invitrogen, D1825) were injected bilaterally into the region of D1–D3 representation in S1 and/or motor cortex. All injections (6–9 per hemisphere and always an identical number bilaterally in any one monkey), were made using a constant pressure Hamilton syringe (20μl capacity) with a tapered glass micropipette attached (tip diameter ≤ 30 μm) with 5 minute epoxy. Each injection delivered 0.3μl of tracer into the cortex at a 1 mm depth, and the pipette was kept in position for 1 minute before being removed and retested.

BDA was visualized in axon terminals histochemically, with the attachment of peroxidase (ABC kit, Vector, PK-6100), and the chromagen diaminobenzidine (DAB, Sigma). Tissue sections were cut coronally using a freezing microtome (50μm) and collected and washed in 0.1M PB (phosphate buffer, pH 7.4), incubated in ABC for 1 h, rinsed, pre-incubated in nickel intensified (0.04% $NiNH_4$) diaminobenzidine (0.05% DAB) in 0.1M PB, and finally incubated with the same solution with 0.01% H_2O_2 until the reaction product was clearly visible (8–10 minutes).

Lucifer Yellow dextran (LYD) was visualized with immunohistochemistry. Tissue sections were incubated (4°C) with primary anti-Lucifer Yellow (48h, Invitrogen, A-5750, 1:200), a secondary antibody – biotinylated anti-rabbit (24 h, Vector, BA-1000), avidin biotin to attach peroxidase (ABC kit, Vector, PK-4000), and reacted with the chromagen DAB (0.05%) plus 0.01% H_2O_2, 24h later. Details have also been reported previously (Darian-Smith et al., 1999).

Pathway Analysis

The spinal cord was sectioned coronally (50μm) through C5-T1 and a series of sections taken every 300–400μm for histochemical and immunohistochemical processing to visualize BDA and LYD. An additional series was stained for cresyl violet.

Distribution territories were defined as the region occupied by the distribution of terminals labeled by an injection into the D1–D3 representation (as defined electrophysiologically) in somatosensory or motor cortex. LYD and BDA labeled terminal boutons were mapped within the spinal grey matter using the tracing system Neurolucida (MicroBrightField, Inc), and areas were measured for each terminal bouton distribution within a sequential series of coronal sections through C5-T1. A line was drawn around the mapped terminal clusters of labeled boutons, and the area enclosed by this border measured by two different

investigators blind to the side and details of the animal. The mean area was then multiplied by the interval distance to the next slide (0.3 – 0.4 mm), and the sequential volumes summed to give the terminal distribution territory. NeuroExplorer (MicroBrightField, Inc) was used for analyzing areas, and Stereo Investigator software (MicroBrightField, Inc) for 3-dimensional reconstruction of these territories in the spinal cord of one monkey (see Figure 4). Outlying boutons were observed on both sides of the spinal cord, but were not included in the analysis, since they represented less than 1% of the population. If a clump of (≥5 boutons) were observed more than 100μm from other labeled boutons, a separate contour was drawn around this clump and the area added to the larger contour area.

The measurement of axon terminal densities is not an accurate measure, since this process involves the comparison of populations of axon terminals labeled with cortical injection series that were made into different hemispheres. The relative uptake and transport of the label from the different injection series cannot be measured, so results from this type of analysis are not reliable and can only be used as a broad stroke descriptor, and to define density changes along the rostro-caudal axis on each side of the spinal cord. For this reason, no attempt was made to use sterelogy in this assessment, since the differences noted were descriptive, largescale, and a full stereological approach would have in no way altered the observations. Given these caveats, we measured terminal bouton densities for 8 injection series (4 somatosensory and 4 motor), to determine any consistent patterns, both rostrocaudally and bilaterally. All labeled terminals were mapped in these animals and their terminal density was taken as the total number of boutons mapped within the spinal gray matter, both within sections and through the rostrocaudal series of sections. All sections were cut at 50μm thick and were separated by either 300 or 400μm with the interval consistent within the animal.

Statistical Analysis

The 7 monkeys yielded 10 different section series – 5 for each corticospinal projection; and 5 for each tracer, approximately balanced across the two projections. Each section in a series provided an ipsilateral and contralateral data point. These data were treated as a nested repeated measures design, implemented as a Restricted Maximum Likelihood (REML) mixed model repeated measures general linear model (GLM) in JMP 9 for Windows. The analysis was blocked by section number (as a fixed effect), that was nested within section series. Section series was treated as a random effect blocking factor (to accommodate appropriate error terms for the repeated measures design; Newman et al.,1997) nested within tracer and corticospinal projection (i.e. as crossed between-subject factors). Side (contra- *vs* ipsi- lateral) was included as a crossed within-subject factor. All interactions were included to test for any effect of tracer, and to calculate the appropriate error terms for a mixed model (Newman et al., 1997). The factor of interest is the side x corticospinal projection interaction – which tests whether the difference between sides differs between the projections. Post hoc planned contrasts and Tukey tests were used to further investigate this factor. Type III sums of squares ensured that all effects were tested once the influence of all other effects was taken into account. The assumptions of GLM (homogeneity of variance, normality of error, and linearity), were confirmed post hoc following Grafen and Hails (2002), and the data square-root transformed to meet these assumptions.

Although some monkeys are represented by two section series, we chose to use section series as the unit (because each series uses a different tracer and/or represents a different corticospinal projection). In initial analyses we confirmed that our results held up if we excluded section series that came from the same monkey. Therefore, because our results were the same regardless of whether we used both injection series from monkey M1108, here we present the full data. As described above, all monkeys received an injection series (either LYD or BDA) in both motor and somatosensory cortex, other than M1108 (which

received both LYD and BDA injection series in motor cortex). Three of the BDA series were excluded due to a faulty batch from the manufacturer.

All figures were assembled and created in CorelDraw X4 (Ottawa, Canada), and photomicrographs altered for contrast and brightness within this program.

RESULTS

Corticospinal projections originating in S1 (5 projections in 5 monkeys) and primary motor cortex (5 projections in 4 monkeys), were analyzed in a total of 7 monkeys (see Table 1 for details). Injections were always made bilaterally in the region of hand and digit (D1–D3) representation that was identified electrophysiologically for accurate injection placement (Figure 1). Where injections were placed contralateral to the lesion, this was the region undergoing reorganization (Darian-Smith and Brown, 2000).

To ensure that labeling did not occur in response to changes in membrane uptake properties following injury, both BDA and LYD were used in different animals in the S1 and primary motor cortex. Previous reports of this phenomenon have shown different labeling for horseradish peroxidase (HRP) in neurons whose axons were damaged in some way. However, in the present study, HRP was not used, and the neuron populations labeled were many synapses removed from the injury site and were not directly damaged by the injury. In addition, the terminal labeling we observed from both cortices and tracers in the spinal cord contralateral to the lesion, was consistent with previous reports for normal animals (Ralston and Ralston, 1985; Galea and Darian-Smith, 1994), and equivalent for the two tracers used (see M1108). The ‘ectopic’ labeling from motor cortex observed in 3 of 4 motor CST animals, and described below, was also in a region that has not been previously described. Our statistical analysis also controlled for confounds due to tracer and confirmed that there was no tracer related effect in the data. For these reasons, tracer uptake anomalies were not considered a concern in the present study.

In each animal, the region analyzed involved the ‘lesion zone’ or that region of the spinal cord corresponding to the rostrocaudal extent of the dorsal rhizotomy. We were able to determine the boundaries of this region very accurately during spinal cord dissection, since the cut rootlets and dorsal root entry to the cord, were clearly visible. Terminal field boundaries were drawn around labeled bouton populations in a series of spinal sections, and the distribution volumes calculated. Table 1 gives the percentages of the ipsilateral/ contralateral terminal territory volumes.

Terminal territory statistical measures

Neither the tracer main effect, nor the tracer-by-projection, the tracer-by-side, or the tracer-by-side-by-group interactions were significant, which indicates that the tracer had no effect on the outcome. By contrast the projection-by-side interaction was significant (REML mixed model: $F_{1,6.141} = 28.7260$; $P = 0.0016$). Post hoc Tukey tests, and planned contrasts revealed that this was due to no difference in area between sides in the motor corticospinal projection group (planned contrast: $F_{1,6.026} = 2.8502$; $P = 0.1421$) *versus* a decrease in ipsilateral terminal field area compared with contralateral field area in sensorimotor corticospinal projections ($F_{1,6.258} = 34.4613$; $P = 0.0009$), see Figure 7).

Corticospinal projection patterns

Projection patterns were consistent across monkeys. Injections were examined through a series of sections (50μm thick, 300 or 400 μm intervals but consistent within each monkey) through the hand representation within the sensorimotor cortex. Though the precise boundaries of these injections were not easily mapped (i.e. the exact zone of uptake of LYD

and BDA is not clearly demarcated), identical injections were made into physiologically identified regions on the two sides of the cortex during the second surgery. Injections were determined not to extend beyond the cortical grey matter or across the central sulcus, which could have compromised the data. Figure 1 shows example of an injection series reconstruction in the somatosensory cortex in M601. Though the exact boundary of the injection sites were not sharply delineated (making reconstruction and volume analysis impossible), injections were always matched precisely for number, volume injected and placement at the time of injection. There were no obvious differences in injection extent between hemispheres in any of the monkeys analyzed, that may have accounted for the differences in terminal labeling observed and described below.

Somatosensory cortex—When anterograde tracers were injected into the primary somatosensory cortex (in D1–D3 representation), the distribution territory of terminal labeling on the lesioned side of the spinal cord was significantly reduced compared with the contralateral side. This indicates that there was a significant loss of input from S1 to the cervical dorsal horn. Although this region had been deprived of its normal input following the DRL, the cortical source of this projection pathway is at least 4–5 synapses and potentially more removed from the site of injury. Figure 2 illustrates a typical example of this S1 CST terminal labeling on the two sides of the cervical cord in M601. In this monkey, BDA was injected into the cortex, and the terminal distribution territory on the lesioned side was 60% of that calculated on thecontralateral side. Electrophysiological recordings within S1 allowed us to demarcate the borders of D1–D3 representation, and in this monkey, 7 injections were made within these confines, bilaterally.

As has been reported previously in normal macaques (Ralston and Ralston, 1985; Galea and Darian-Smith, 1994), input from the non-deprived S1 cortex (areas 3b and 1, D1–3 representation) in our monkeys, terminated in the medial dorsal horn (Rexed layers 1–V1), and extended down into the dorsal portion of the intermediate zone (Figure 2; also see Darian-Smith, 2008, 2009). Following the DRL, terminal labeling ipsilateral to the lesion was still observed in all layers of the dorsal horn, but was diminished in its distribution territory, compared with the contralateral side (see Figure 5). Though the density of terminal boutons cannot be easily quantified when labeling results from two different sets of injections, density overall was also greatly reduced on the side of the lesion (Figures 2 and 6). It is not clear whether the diminished terminal territory was the result of a retraction of axon terminal branches or reflected the attrition or death of neurons.

Motor cortex—In contrast to the pattern of labeling observed from S1 following a DRL, input from the primary motor cortex was not significantly different on the two sides of the spinal cord, but did trend towards being greater on the side of the lesion in 3 of the 4 monkeys examined. That is, within the lesion zone, the grey matter terminal distribution territory was calculated to average 112 ± 20% (s.d.) of that observed on the contralateral (non-lesioned) side. Figures 3 and 4 illustrate the pattern of terminal labeling observed in monkey M604. Terminal labeling within the spinal grey ventral-medial dorsal horn and the dorsolateral ventral horn. This has been well described in the literature in normal macaques (Ralston and Ralston, 1985; Galea and Darian-Smith, 1994) and our findings did not deviate from the expected pattern. However, in the lesion zone on the side of the lesion in 3 of the 4 monkeys, labeled terminal boutons were also mapped within a more dorsal portion of the dorsal horn than was found on the contralateral side (Figures 3), or compared to what has been reported previously. Figure 4 shows a 3-dimensional reconstruction of the terminal territory within the lesion zone in monkey M604, illustrating the region of expansion into the dorsal horn. The extended region is clearly visible within the dorsal horn on the side of the DRL. A photomicrograph of this aberrant labeling is also shown in Figure 6. Taken together, our findings indicate that the motor CST terminal territory was not reduced in size,

and that at least some of the CSTs underwent terminal sprouting into the dorsal horn in response to the DRL.

Importantly, and despite some variability for motor CSTs, the different response of the somatosensory versus the motor cortex projections was robust and highly significant (Figure 7). Figure 5 shows distribution profiles for all somatosensory and motor cortical CSTs. Profiles show terminal areas rostrocaudally and the lesion zone is indicated in each animal. For somatosensory CST projections, ipsilateral areas (red line) were statistically lower than was observed contralaterally. Percentage differences are given for each animal in Table 1.

Terminal bouton density measures

Terminal bouton density maps have little meaning when the tracer injection sets are not identical. That is, there can be a differing uptake from the two sides that might account for the density disparity, rather than it being the result of an actual reduction or increase of the projection. However, in order to at least partially address this issue, we took data from sections that had been mapped and analyzed in 8 injection series (4 for somatosensory and 4 for motor cortex), and quantified the total numbers of labeled boutons mapped on each side through the cervical cord. This analysis was made across all sections mapped rostrocaudally, and not just within the lesion zone. Between 27–31 sections were mapped in each monkey (with total number of boutons in these 7 injection series = 321,399). For projections from the somatosensory cortex, the mean density for the lesion side/contralateral side was 69 % ± 25 % (s.d.) and consistently less on the side of the lesion in all 5 monkeys, whereas for motor cortex, no consistent pattern was observed (mean=93 ± 27%). In all animals the terminal density did change within the ‘lesion zone’ or that region most impacted by the lesion, compared with more rostral and caudal sections. That is, terminal bouton numbers were similar bilaterally through C3–4 sections, and disparities between the sides only became evident in segments C5–C8. This suggests that the density differences observed within the lesion zone were to some extent a result of the lesion and could not be entirely explained by a disparity in the uptake from the injections.

DISCUSSION

Our findings show that over the course of several months following a unilateral cervical DRL, the CST pathways alter in their terminal distribution patterns within the cervical spinal cord in the region most directly affected by the DRL. The CST projection originating in the deprived S1 cortex (in the region representing digits 1–3) retracted axon terminals within the cervical dorsal horn, so that only an average of 56% of the original terminal territory remained. In contrast, the deprived motor cortex CST terminal territory size was not statistically different on the two sides of the cord. However, axon terminal boutons were observed in a region of the dorsal horn beyond their normal domain which indicates terminal sprouting of motor CST axons into this region in response to the lesion. This region of the dorsal horn is known to be greatly impacted by the DRL, so local terminal sprouting into the region likely reflects changes in the local circuitry resulting from the injury.

A number of caveats should be considered in the current analysis. First, the number of animals used was small. This is inherent in any nonhuman primate study, but did not decrease the power of the statistical analysis, which took this, the tracer and other variables into account (see Methods, and for discussion of statistical power and sample size, see Hoenig and Heisy, 2001; Levine and Ensom, 2001). A second point that should be considered in a study of this type has to do with tracer uptake efficacy. The two tracers used, BDA and LYD, were included in the statistical analysis and terminal labeling patterns were not linked with the tracer used. Uptake times for BDA ranged from 6–9 weeks and both the 6 and 9 week time periods produced almost identical terminal territory proportions (60 and

62%, see Table 1). Similarly, for LYD, terminal labeling differences between animals could not be linked with differences in post-injection uptake times (5–7 weeks). Together these findings indicate that the tracers, and uptake times, did not account for the differences observed.

Though it is possible that there was a small amount of shrinkage in the deafferented portion of the spinal cord, we found no evidence of this in a prior study where we measured and compared the two sides following the same lesion to address this point (see Darian-Smith et al., 2010). Within the cortex, reorganization is also unlikely to have altered tracer uptake in any significant way, since cortex was many synapses removed from the injury site and the mediolateral extent and number of injections were equivalent bilaterally in all animals.

The clear difference in the response of CSTs originating from the S1 versus the motor cortex does not preclude local sprouting from S1 CST neurons. Axon terminal sprouting would not be detectable in our analysis if it occurred within the normal terminal territory. Our findings do, however, indicate a significant loss of axon terminals from the dorsal horn CST originating in S1 cortex. It is not known if this results from a retraction of axon terminal branches, or from the loss of entire neurons (see discussion below). It should also be noted that fewer boutons were observed overall on the side of the lesion (compared to the contralateral side) in S1 CSTs, and that a similar number were observed in motor CSTs. These terminal bouton number differences were only observed within the lesion zone, which indicates that they were, at least partly, a result of the lesion.

Why there is such a different post-rhizotomy response of the CSTs originating in the S1 versus the motor cortex is not clear. It is certainly true that each cortical region has a very different functional role, reflected in both the cortical connectivity and spinal termination patterns. Cortical input to the primary somatosensory cortex is restricted to local parietal and motor cortex as well as SII (Darian-Smith et al., 1993), with the primary input to this cortex coming from the spinal cord. S1 CST input to the dorsal horn is thought to provide descending control of sensory input (“sensory reafference”), particularly as it relates to movement (Lemon and Griffiths, 2005). In contrast, the primary motor cortex receives far more complex cortical input from the cingulate motor area, the supplementary motor area, postarcuate cortex, insular cortex and postcentral cortical areas 2 and 5 (Darian-Smith et al., 1993). Its subcortical input comes primarily from the basal ganglia, and cerebellum (by way of the thalamus), and it receives only a tiny input from the spinal cord (via the brainstem and thalamus). The motor CST plays an executive as well as an acquisitive role in coordinated hand and digit movements and it terminates both directly on motor neurons (a uniquely primate feature- for evidence for and against see Alsternak et al., 2004; Yang and Lemon, 2003; Raineteau et al., 2002), and on interneurons synapsing on motor neurons, within the intermediate and dorsal ventral horn.

These differences mean that the DRL directly deprives the dorsal horn and the S1 cortex (D1–D3 representation) of their major source of input. When sensory input is removed from the dorsal horn, sensory reafference is no longer possible, and this presumably results in the retraction of such a large number of S1 CST terminal endings. The primary motor cortex, on the other hand, has only a small spinal input (via the thalamus) that is lost, so CST neurons are more likely to respond to alternate coherent connections that may have played a lesser functional role pre-lesion. In addition, in the spinal cord, normal input to the intermediate zone is not within the epicenter of lost afferent input (i.e. the dorsal horn). This suggests that the motor CST has a far greater capacity to reorganize following a DRL than the S1 CST.

It is also unlikely that a loss of CST neurons from somatosensory cortex accounts for the different CST responses. Our electrophysiological mapping both here and in previous

studies does not show discernible shrinkage of the reorganizing region (4–6mm diameter) of the somatosensory cortex, and injections were always made over an equivalent region bilaterally. Studies unrelated to this one indicate remodeling of the circuitry in the region, and a mild immune proliferative response, but there is little evidence of neuronal loss at 1–5 months following the lesion, at a level that could account for the changes in the CSTs observed (Darian-Smith and colleagues, unpublished). This is unsurprising, given that the lesion is at least 3–4 synapses removed from the somatosensory cortex, and other inputs (e.g. from the thalamus, basal ganglia, ipsi- and contralateral cortex, etc.) would still be salient and active in what is a relatively small region of cortex.

Our study differs from earlier investigations looking at CST plasticity following spinal injury in that the DRL occurs outside the spinal cord and outside the central nervous system, and CSTs are not directly injured. A DRL removes all sensory input from a specific part of the body, while a hemisection partially removes sensory input from the body caudal to the injury, but leaves the spinothalamic tract almost entirely intact. A hemisection also cuts approximately 90% of the descending CST but leaves a smaller 8–10% ipsilateral component intact. Following a hemisection, collateral branches that normally cross the midline from the ipsilateral CST projection play a significant role in the reorganization that takes place, as these axons are spared by the lesion (Ralston and Ralston, 1985; Galea and Darian-Smith, 1994, 1995; Rosenzweig et al., 2009). The role of these collaterals in the present study is not known, though they are unlikely to play a dominant role since the CSTs are not themselves injured. In these ways, the hemisection studies cannot be directly compared with our current work. However, they do highlight the capacity for spontaneous localized sprouting and plasticity in spared CST fibers (Galea and Darian-Smith, 1997a; Rosenzweig et al., 2010), and underscore the critical importance of the CST pathway in the recovery of hand and digit function following spinal injury.

How the circuitry reorganizes at the synaptic level following any spinal injury is not well understood. Our own studies show that in the course of several months following a cervical DRL, during a period of behavioral recovery in the hand (Darian-Smith and Ciferri, 2005), spared primary afferent fibers sprout locally within the spinal dorsal horn to presumably connect with postsynaptic neurons that have lost their normal input (Darian-Smith, 2004). At the ultrastructural level, on the side of the lesion, ~85% of primary afferent terminals are lost during the same period, but there is a dramatic increase in inhibitory synaptic profiles, including a more than 3-fold increase in GABAergic synaptic profiles in the dorsal horn (Darian-Smith et al., 2010). This may correspond to local sprouting of interneurons, and may also reflect the formation of new interneurons in the deprived region (Vessal et al., 2007). In the same study (Darian-Smith et al., 2010), CST fibers labeled from the S1 cortex were also shown to receive synapses from the dendrites of local GABAergic interneurons in the deprived dorsal horn. Such dendro-axonal connections are not known in normal animals (Ralston and Ralston, 1985), and support the possibility that inhibitory connections play a major role in the formation of new circuitry in the dorsal horn following a DRL.

Though much remains unknown, it is possible to hypothesize about some of the changes that occur within the dorsal horn, based on what we do know. The DRL in our animals removes most of the sensory input to the dorsal horn but not all, as we have shown previously (Darian-Smith, 2004). This leads to a retraction of CST terminals from the more severely deprived S1 CST fibers, but not from CST fibers originating in the primary motor cortex. Localized sprouting of the remaining mostly motor CST terminals occurs at the same time that spared primary afferents sprout locally within the dorsal horn (Darian-Smith, 2004). We observe changes in the termination patterns of the motor CST fibers because they occur outside their normal territory, and because these cells maintain more diverse connections within the intermediate zone. This may allow them to play a greater role in establishing new

circuitry within the dorsal horn during this period. The increase in inhibitory connections within the dorsal horn is also likely to contribute to the formation and stabilization of circuitry within this region, as previously described (Darian-Smith et al., 2010).

Sensorimotor interactions that occur within the spinal cord following spinal nerve or cord injury have long been recognized (Goldberger and Murray, 1974; Li et al., 2002; Sheth et al., 2002; Rossignol et al., 2008), and our findings in this paper further highlight how little we still understand of these interactions, particularly in the primate.

Future studies will be important in deciphering the details of the corticospinal contribution to circuit reorganization within the spinal cord over an early and chronic timeframe. It will also be important to consider the contribution of CST projections from other cortical regions (i.e. other frontal, cingulated and posterior parietal regions), and the role each CST plays in the recovery of hand function.

Acknowledgments

Support: We would like to thank Dr Karen-Amanda Irvine for helpful comments on the manuscript, and Dr Joseph Garner for his statistical expertise. This work was supported by grants from the Roman Reed State Funds for Spinal Cord Injury (RR07-199) and the NIH NINDS (RO1 NS048425).

REFERENCES CITED

Alsternak B, Ogawa J, Isa T. Lack of monosynaptic corticomotoneuronal EPSPs in rats: disynaptic EPSPs mediated via reticulospinal neurons and polysynaptic EPSPs via segmental interneurons. J Neurophysiol. 2004; 91:1832–1839. [PubMed: 14602838]

Brus-Ramer M, Carmel JB, Chakrabarty S, Martin JH. Electrical stimulation of spared corticospinal axons augments connections with ipsilateral spinal motor circuits after injury. J Neurosci. 2007; 27(50):13793–13801. [PubMed: 18077691]

Case LC, Tessier-Lavigne M. Regeneration of the adult central nervous system. Curr Biol. 2005; 15 (18):R749–753. [PubMed: 16169471]

Darian-Smith C, Darian-Smith I, Burman K, Ratcliffe N. Ipsilateral cortical projections to areas 3a, 3b, and 4 in the macaque monkey. J Comp Neurol. 1993; 335(2):200–13. [PubMed: 8227514]

Darian-Smith I, Galea MP, Darian-Smith C, Sugitani M, Tan A, Burman K. The anatomy of manual dexterity. The new connectivity of the primate sensorimotor thalamus and cerebral cortex. Adv Anat Embryol Cell Biol. 1996; 133:1–140. [PubMed: 8854379]

Darian-Smith C, Tan A, Edwards S. Comparing thalamocortical and corticothalamic microstructure and spatial reciprocity in the macaque ventral posterolateral nucleus (VPLc) and medial pulvinar. J Comp Neurol. 1999; 410:211–34. [PubMed: 10414528]

Darian-Smith C. Primary afferent terminal sprouting after a cervical dorsal rootlet section in the macaque monkey. J Comp Neurol. 2004; 470(2):134–150. [PubMed: 14750157]

Darian-Smith, C. Plasticity of somatosensory function during learning, disease and injury. In: Gardner, Esther; Kaas, Jon H., editors. The Senses: A Comprehensive Reference. Vol 6, Somatosensation. San Diego: Academic Press; 2008. p. 259-298.

Darian-Smith C. Synaptic plasticity, neurogenesis, and functional recovery after spinal cord injury. Neuroscientist. 2009; 15:149–165. [PubMed: 19307422]

Darian-Smith C, Brown S. Functional changes at periphery and cortex following dorsal root lesions in adult monkeys. Nature Neuroscience. 2000; 3(5):476–481.

Darian-Smith C, Ciferri M. Loss and recovery of voluntary hand movements in the macaque following a cervical dorsal rhizotomy. J Comp Neurol. 2005; 491(1):27–45. [PubMed: 16127695]

Darian-Smith C, Ciferri M. Cuneate nucleus reorganization following cervical dorsal rhizotomy in the macaque monkey: its role in the recovery of manual dexterity. J Comp Neurol. 2006; 498(4):552–565. [PubMed: 16874805]

Darian-Smith C, Hopkins S, Ralston HJ 3rd. Changes in synaptic populations in the spinal dorsal horn following a dorsal rhizotomy in the monkey. J Comp Neurol. 2010; 518(1):103–117. [PubMed: 19882723]

Galea MP, Darian-Smith I. Multiple corticospinal neuron populations in the macaque monkey are specified by their unique cortical origins, spinal terminations, and connections. Cerebral Cortex. 1994; 4:166–194. [PubMed: 8038567]

Galea MP, Darian-Smith I. Postnatal maturation of the direct corticospinal projections in the macaque monkey. Cereb Cortex. 1995; 5:518–540. [PubMed: 8590825]

Galea MP, Darian-Smith I. Corticospinal projection patterns following unilateral section of the cervical spinal cord in the newborn and juvenile macaque monkey. J Comp Neurol. 1997a; 381(3): 282–306. [PubMed: 9133569]

Galea MP, Darian-Smith I. Manual dexterity and corticospinal connectivity following unilateral section of the cervical spinal cord in the macaque monkey. J Comp Neurol. 1997b; 381:307–319. [PubMed: 9133570]

Garcia-Alias G, Barkhuysen S, Buckle M, Fawcett JW. Chondroitinase ABC treatment opens a window of opportunity for task-specific rehabilitation. Nat Neurosci. 2009; 12(9):1145–1151. [PubMed: 19668200]

Ghosh A, Haiss F, Sydekum E, Schneider R, Gullo M, Wyss MT, Mueggler T, Baltes C, Rudin M, Weber B, Schwab ME. Rewiring of hindlimb corticospinal neurons after spinal cord injury. Nat Neurosci. 2010; 13:97–104. [PubMed: 20010824]

Goldberger ME, Murray M. Restitution of function and collateral sprouting in the cat spinal cord: the deafferented animal. J Comp Neurol. 1974; 158:37–54. [PubMed: 4430736]

Grafen, A.; Hails, R. Modern statistics for the life sciences. Oxford & New York: Oxford University Press; 2002.

Hoenig JM, Heisey DM. The abuse of power: The pervasive fallacy of power calculations for data analysis. Am Stat. 2001; 55:19–24.

Lemon RN. Descending pathways in motor control. Annu Rev Neurosci. 2008; 31:195–218. [PubMed: 18558853]

Lemon RN, Griffiths J. Comparing the function of the corticospinal system in different species: organizational differences for motor specialization? Muscle Nerve. 2005; 32(3):261–79. [PubMed: 15806550]

Levine M, Ensom MHH. Post hoc power analysis: An idea whose time has passed? Pharmacother. 2001; 21:405–409.

Li L, Xian CJ, Zhong JH, Zhou XF. Effect of lumbar 5 ventral root transection on pain behaviors: a novel rat model for neuropathic pain without axotomy of primary sensory neurons. Exp Neurol. 2002; 175:23–34. [PubMed: 12009757]

Liu K, Lu Y, Lee JK, Samara R, Willenberg R, Sears-Kraxberger I, Tedeschi A, Park KK, Jin D, Cai B, Xu B, Connolly L, Steward O, Zheng B, He Z. PTEN deletion enhances the regenerative ability of adult corticospinal neurons. Nat Neurosci. 2010; 13(9):1075–1081. [PubMed: 20694004]

Newman JA, Bergelson J, Grafen A. Blocking factors and hypothesis tests in ecology: Is your statistics text wrong? Ecology. 1997; 78(5):1312–1320.

Raineteau O, Fouad K, Bareyre FM, Schwab ME. Reorganization of descending motor tracts in the rat spinal cord. Eur J Neurosci. 2002; 16(9):1761–71. [PubMed: 12431229]

Ralston DD, Ralston HJ III. The terminations of corticospinal tract axons in the macaque monkey. J Comp Neurol. 1985; 242:325–337. [PubMed: 2418074]

Rosenzweig ES, Brock JH, Culbertson MD, Lu P, Moseanko R, Edgerton VR, Havton LA, Tuszynski MH. Extensive spinal decussation and bilateral termination of cervical corticospinal projections in rhesus monkeys. J Comp Neurol. 2009; 513(2):151–163. [PubMed: 19125408]

Rosenzweig ES, Courtine G, Jindrich DL, Brock JH, Ferguson AR, Strand SC, Nout YS, Roy RR, Miller DM, Beattie MS, Havton LA, Bresnahan JC, Edgerton VR, Tuszynski MH. Extensive spontaneous plasticity of corticospinal projections after primate spinal cord injury. Nat Neurosci. 2010; 13 (12):1505–1510. [PubMed: 21076427]

Rossignol S, Barrière G, Frigon A, Barthélemy D, Bouyer L, Provencher J, Leblond H, Bernard G. Plasticity of locomotor sensorimotor interactions after peripheral and/or spinal lesions. Brain Res Rev. 2008; 57:228–40. [PubMed: 17822774]

Sheth RN, Dorsi MJ, Li Y, Murinson BB, Belzberg AJ, Griffin JW, Meyer RA. Pain. 2002; 96:63–72. [PubMed: 11932062]

Vessal M, Aycock A, Garton MT, Ciferri M, Darian-Smith C. Adult neurogenesis in primate and rodent spinal cord: comparing a cervical dorsal rhizotomy with a dorsal column transection. Eur J Neurosci. 2007; 26(10):2777–2794. [PubMed: 18001275]

Vessal M, Darian-Smith C. Adult neurogenesis occurs in primate sensorimotor cortex following cervical dorsal rhizotomy. J Neurosci. 2010; 30(25):8613–8623. [PubMed: 20573907]

Yang HW, Lemon RN. An electron microscopic examination of the corticospinal projection to the cervical spinal cord in the rat: lack of evidence for cortico-motoneuronal synapses. Exp Brain Res. 2003; 149:458–69. [PubMed: 12677326]

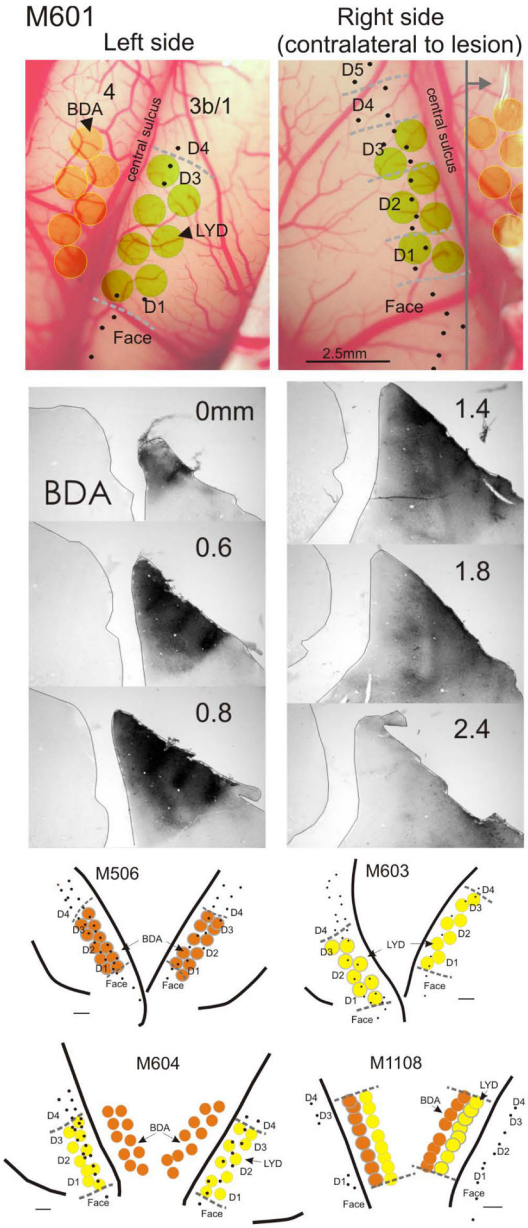

Figure 1.

Examples of cortical mapping and neuronal tracer placement and reconstruction, in monkeys M601, M506, M603, M604, and M1108. In M601, which was typical, extracellular recordings were made in the right (deprived) cortex first, and the hand mapped (dashed gray lines) to determine boundaries for digits 1–3 (D1–D3). Fewer recordings were made in this animal on the left side, since we were only interested in determining D1 and D3 borders for injection placement. Equivalent injections were made bilaterally, and those in motor cortex were placed according to somatosensory cortex recordings. Sections were processed through all injections to ensure that white matter was not involved and that there was no cross sulcus contamination. There was no visible damage or necrosis observed at the injection sites within any cortical injection series. A series of sections in M601 through the BDA injections on the right side are shown. Gray vertical line in upper right image indicates the coronal

plane of the BDA section series. Individual injection site volumes were not estimated, given poor definition of the injection borders of the tracers LYD and BDA. However, injections were found to be equivalent in size and placement across animals. Lower maps show additional examples. Scale bar in lower images = 1mm.

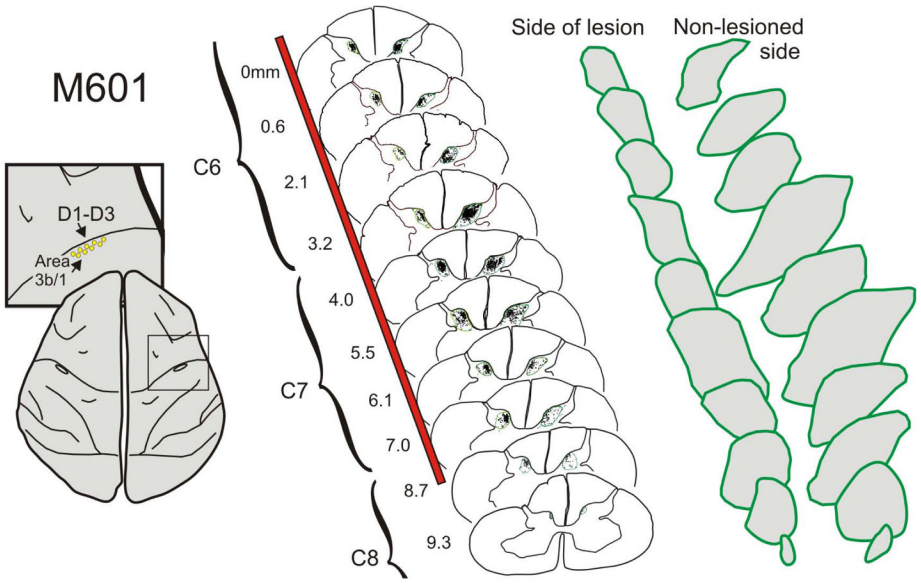

Figure 2.

Example of corticospinal terminal labeling within the cervical spinal cord, that originated from the somatosensory cortex (D1–3 representation). Injections for this animal are shown in detail in Figure 1. Terminal boutons were mapped in a series of sections (10 illustrated, 36 total) through the lesion zone (that region directly involved by the lesion). A boundary was drawn around the distributions, which are enlarged to the right. Bouton distribution territories were found to be significantly smaller on the side of the lesion, compared to the contralateral side. This was consistent across monkeys. Red bar indicates extent of lesion.

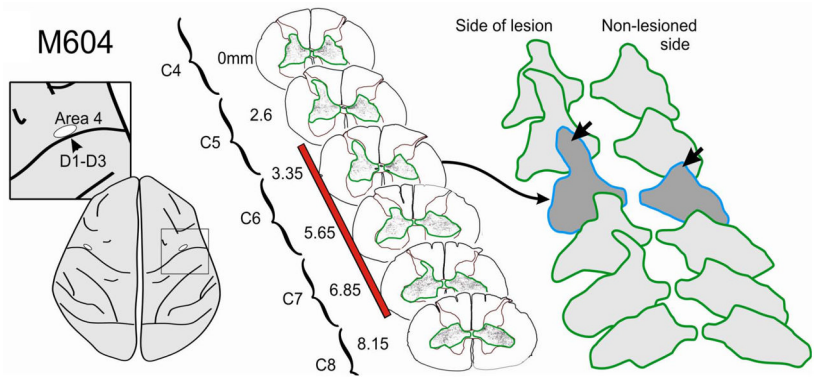

Figure 3.

Example of corticospinal terminal labeling within the cervical spinal cord, that originated from the primary motor cortex (D1–3 representation). Terminal boutons were mapped in a series of sections (6 illustrated, 52 total) through the lesion zone. In contrast to somatosensory cortex projections, bouton distribution territories from motor cortex were not significantly larger on the side of the lesion, compared to the contralateral side, even though there was a trend in this direction in 3 of the 4 monkeys examined. However, independent of the overall territory measure, terminal boutons were observed in 3 of the 4 monkeys in a region of the dorsal horn not normally associated with the motor cortex. This is a region most directly impacted by the DRL. Red bar indicates extent of lesion.

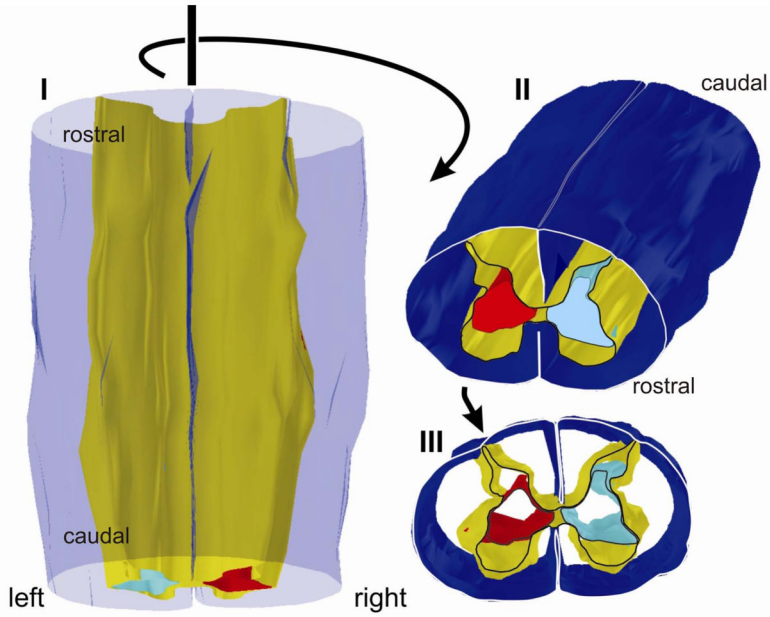

Figure 4.

Three dimensional reconstruction of the corticospinal projection from primary motor cortex (Area 4) in monkey M604 (Figure 3) seen from a dorsal (I), rostro-dorsal (II), and rostral (III) perspective. Pial surface is transparent blue in I and dark blue in II and III. Gray matter is shown in yellow. Only outlines are rendered rostrocaudally so that image is hollow cylindrical form. The lesion was made on the left side, and the aberrant dorsal extension of the terminal territory on the left side is clearly visible (light blue). The terminal territory on the side contralateral to the lesion is rendered in red. Only the most rostral section is outlined.

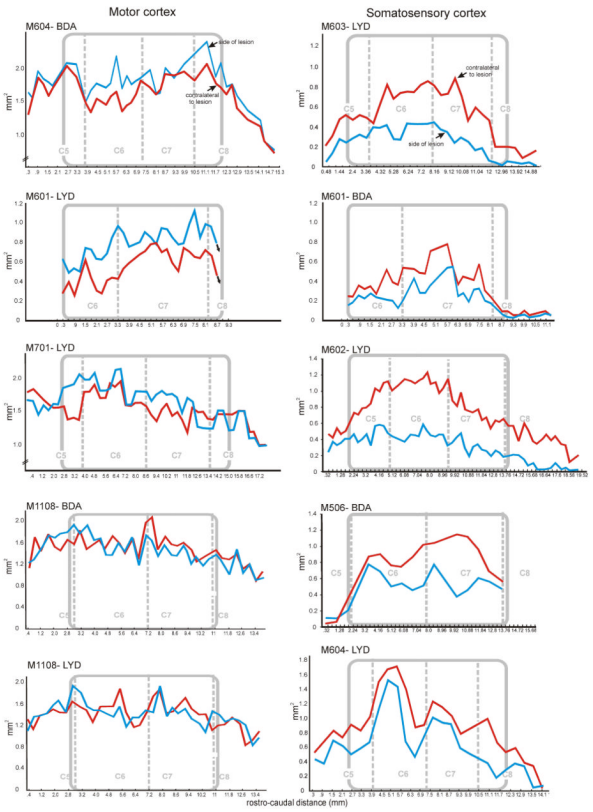

Figure 5.

Terminal distribution histogram profiles, comparing primary motor and somatosensory CST projection patterns in all animals. Territory areas for each section are indicated on the Y abscissa, and volumes were calculated per section (x interval to next section). Section number is shown on the X abscissa. Gray rectangles demarcate the rostrocaudal extent of the lesion (the lesion zone), relative to the cervical segments. Terminal territories (red line) were consistently smaller on the ipsilateral side compared to the contralateral side (blue line) for somatosensory CST projections. In contrast, and overall, the motor CST projection territories were not significantly different on the two sides of the cord. The average percentage differences are given in Table 1.

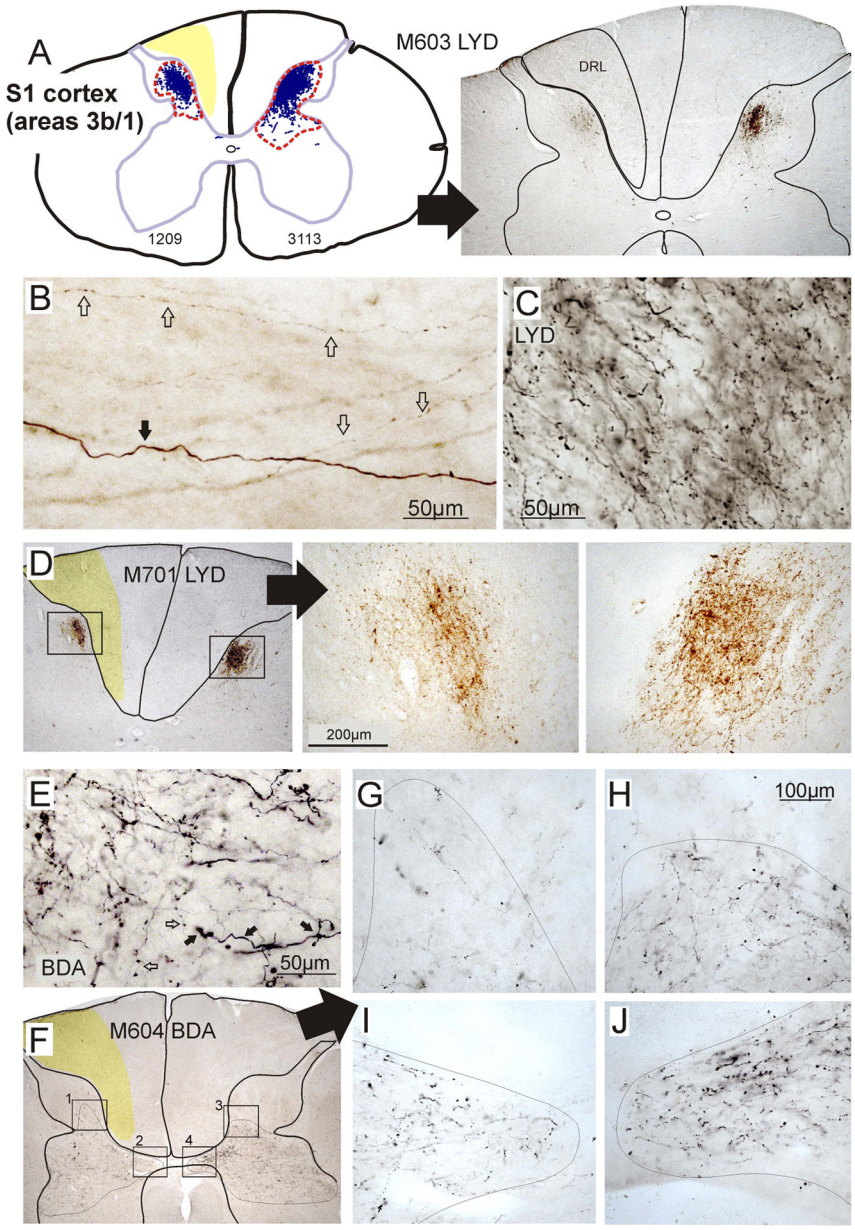

Figure 6.

Photomicrographs and maps showing typical labeling patterns of corticospinal projections from somatosensory (a–e), and motor cortex (f) to the cervical spinal cord. ***A–D*** shows examples of LYD terminal labeling from primary somatosensory cortex. The red dotted line in ***a*** (left image) outlines the terminal distributions in this section. The region of degeneration in the cuneate fasciculus of the dorsal column is indicated in yellow (***A, D, F***) or outlined (***a*** right). ***B–C*** shows LYD labeling at a higher magnification. Labeled large (black arrow) and small (white arrows) caliber axons were observed in all sections and with both tracers. Note in ***b*** that small caliber axons frequently had boutons *en passant*. The two different morphologies indicate different conductance velocities and functional properties, and (**E**) shows correspondingly large (black arrows) and small (white arrows) boutons associated with these corticospinal axons. ***E–F*** shows BDA labeling and an example of a

motor corticospinal projection in M604. ***F*–*G*** illustrates an aberrant region of sprouting ipsilateral to the lesion which was observed in the dorsal horn in 3 of 4 monkeys with labeled motor CSTs. Additional regions of labeling are also enlarged in ***H*–*J*** for comparison of the two sides.

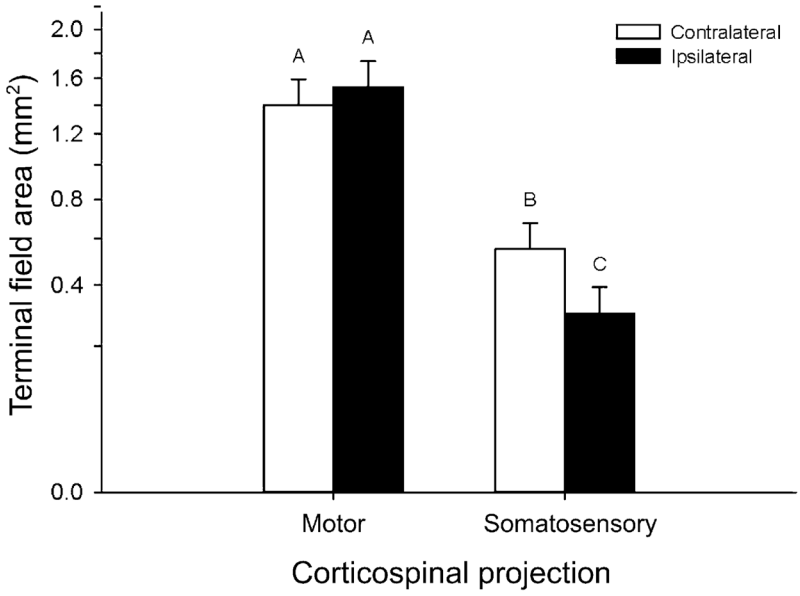

Figure 7.

Mean terminal field areas ipsilateral and contralateral to the lesion, for primary motor and S1 CST projections. Error bars are standard errors. Data were square-root transformed for analysis, and are displayed in transformed space, with real-world units on the y-axis. Superscripts above the means indicate means which do not differ significantly as determined by a Tukey test for multiple comparisons. Motor CST projections showed no difference between the sides of the cord overall, while somatosensory CST projections showed a marked decrease on the ipsilateral side of the cord.

Table 1

Details of monkeys used in the present study, showing weight, postoperative times, anterograde tracer used and placement of tracer, and terminal distribution territories or volumes calculated as percentage of the ipsi/contra side volumes. All calculations were made inside the lesion zone, as indicated in Figure 5.

Monkey ID	mean weight (kg)	Post-operative times (wks) -time between 1st & 2nd surgery -time for tracer uptake	Tracer and cortical placement		% ipsi/contra terminal volume	
			Somatosensory	Motor	Somatosensory	Motor
M506	4.02	14 9	BDA		62%	
M601	3.00	9.5 6	BDA	LYD	60%	145%
M602	3.04	9 6	LYD		39%	
M603	2.50	11 7	LYD		46%	
M604	2.02	14 7	LYD	BDA	72%	110%
M701	3.14	18 5		LYD		112%
M1108	2.62	15 7		BDA LYD		99% 98%
				mean (± s.d.)	55.8 ± 13%	112.8 ± 20%